Measurement 87 (2016) 74–82

Contents lists available at ScienceDirect

Measurement

journal homepage: www.elsevier.com/locate/measurement

Rotating-coil calibration in a reference quadrupole, considering roll-angle misalignment and higher-order harmonics

P. Arpaia [a,b,*], M. Buzio [b], O. Köster [c,b], S. Russenschuck [b], G. Severino [d,b]

[a] Department of Electrical Engineering and Information Technology, University of Naples Federico II, Naples, Italy
[b] Technology Department, European Organization for Nuclear Research (CERN), Geneva, Switzerland
[c] Technical University of Darmstadt, Darmstadt, Germany
[d] Department of Engineering, University of Sannio, Benevento, Italy

ARTICLE INFO

Article history:
Received 7 August 2015
Received in revised form 5 November 2015
Accepted 16 February 2016
Available online 4 March 2016

Keywords:
Coils, induction
Sensors magnetic field
Calibration
Measurement of magnetic field
Magnetic field in electromagnetism

ABSTRACT

A method is proposed for calibrating the radius of a rotating coil sensor by relaxing the metrological constraints on alignment and field errors of the reference quadrupole. A coil radius calibration considering a roll-angle misalignment of the measurement bench, the magnet, and the motor-drive unit is analyzed. Then, the error arising from higher-order harmonic field imperfections in the reference quadrupole is assessed. The method is validated by numerical field computation for both the higher-order harmonic errors and the roll-angle misalignment. Finally, an experimental proof-of-principle demonstration is carried out in a calibration magnet with sextupole harmonic.

1. Introduction

In particle accelerators, magnetic measurements are necessary for establishing a suitable experimental coherence among machine requirements, beam physics simulations, and magnet development [2]. Beam physicists allocate a suitable budget for magnet misalignment and require experimental magnetic field maps pointing out the field errors (expressed as *multipoles* [3]). During magnet prototyping, measurements allow also design calculations, material properties, and fabrication methods to be verified [4]. Fields are measured also for monitoring the magnet behavior online; thus direct feedback to the accelerator control is provided for adjusting the beam bending and for tuning the acceleration parameters.

Based on these depicted findings, different measurements techniques are employed, based on various sensing elements, such as induction coils, oscillating wires, and Hall probes, among others [5,6]. The induction coil is based on the Faraday's law of induction, where the sensing element [7] is turned inside the magnet's aperture in order to provide a spatial harmonic description of the field (*harmonic coil* [3]). A coil consists of several rectangular loops of conducting wire, usually stretched during the winding on a rigid core and then glued to assure a well-defined and stable geometry. Coils can be manufactured by traditional winding methods or printed-circuit board (PCB) [8] technology. The latter is especially suited for small-aperture magnets [9].

Manufacturing errors leading to deviations from the ideal design exist in both the technologies. For the PCBs, a misalignment between layers of different radii is typical. Therefore, an accurate calibration is needed: Several physical parameters of the coil, such as rotation radius, coil area, phase angle, tilt, number of turns, and opening angle

* Corresponding author at: Department of Electrical Engineering and Information Technology, University of Naples Federico II, Naples, Italy.
E-mail address: pasquale.arpaia@unina.it (P. Arpaia).

http://dx.doi.org/10.1016/j.measurement.2016.02.061
0263-2241/

have to be measured carefully in order to reach the required metrological target.

The calibration based on a reference quadrupole magnet [1] is currently used in rotating coil systems. The magnetic-equivalent rotation radius can be obtained in a reference quadrupole field either by measuring the focusing strength, or rotating the coil by a given angle [1] or also before and after a translation in the horizontal (xz) and vertical (yz) planes.

The calibration assumes that the coil and the reference magnet axes are perfectly aligned, limiting the mathematical analysis to two dimensions. However, if significant roll and swing misalignment errors are present, this gives rise to significant calibration errors. Moreover, the equations used to calculate the radius is based on the *feed-down* effect from the quadrupole component [1], by assuming all the contributions of higher-order terms as negligible. This is justified because the dominant field component in the reference magnet is much larger than the field errors of higher-order multipoles [10]. However, if this assumption is not verified, a sextupole magnet is used as reference, or an in-situ calibration is carried out in a nonideal magnet, significant errors arise. Therefore, a reference magnet with stringent metrological constraints of harmonic field quality and alignment is required. This is difficult to achieve, however, for small-apertures or rare-earth permanent magnets.

In this paper, a method is analyzed for calibrating the rotation radius of coils using a reference quadrupole magnet with a higher-order harmonic error, or a misalignment with the coil axis. In particular, in Section 2, the presence of a roll-angle misalignment between the coil axis and the reference magnetic field axis, and higher-order harmonics of the reference quadrupole is analyzed. In Section 3, the effect of coil radius calibration in a quadrupole with a sextupole or octupole error component is simulated numerically by using the field computation program ROXIE [3]. In Section 4, experimental results for validating the proposed method are given.

2. Calibration method

In the following, the two cases of radius calibration are analyzed for rotating coils using a nonideal reference quadrupole having (i) *roll-angle misalignment*, or (ii) *higher-order harmonics*.

2.1. Radius calibration considering roll-angle misalignment

The rotating-coil radius is calibrated by means of two measurements, taken at two different positions of the coil inside a reference quadrupole magnet. The following hypotheses are assumed about the set up and the measurement method:

* The reference quadrupole magnet has a cylindrical symmetry along the longitudinal axis z defining the global reference frame $\{x, y, z\}$.
* The misalignment of the reference quadrupole is modeled as a rotation (roll) around the z axis, without any component of pitch and yaw. The effect on the calibration error of higher-multipole field errors in the reference magnet is neglected, an assumption that will be challenged in the next section.
* Possible misalignment errors among the reference magnet, the coil support, and the displacement stages remain constant between the two measurements. This is a reasonable assumption, owing to the solid structure of the support posts and tables.
* The angular encoder of the rotating coil system (rigidly mounted between the driving system and the coil) is ideal, except for a rotation uncertainty φ_e.
* Between the two measurements, the coil is supposed to be purely translated on the magnet section with respect to the global reference frame from an initial position in the complex plain $z = x + iy$ by $\Delta z = z_b - z_a$ ($|\Delta z| = d$), without loss of generality, the displacement of the harmonic coil is assumed to be confined to the horizontal plane of the reference magnet, hence Δz coincides with Δx. The distance d is known with an uncertainty of ± 0.01 mm.

Let us consider only a transverse section of the measurement setup in the global 2D reference frame $\{x, y\}$ and the frames shown in Fig. 1:

* *Gravity frame*: $\{x_h, y_h\}$, used as external reference, and ideally coincident with the global reference frame $\{x, y\}$;
* *Magnet frame*: $\{x_m, y_m\}$, misaligned by the angle φ_m with the magnet geometric frame which is (not shown in Fig. 1 for the sake of clarity) defined according to the physical dimensions of the magnet, and supposed here as coincident with the gravity frame;
* *Coil Frame*: $\{x_c, y_c\}$, related also to the coils polarity, (represented in Fig. 1 as $\{x_a, y_a\}$ and $\{x_b, y_b\}$ for the two measurements, centered at z_a and z_b, respectively), and misaligned by the angle φ_a with respect to the gravity frame $\{x_h, y_h\}$;
* *Shaft Frame*: $\{x_s, y_s\}$: related to the shaft which supports the coil assembly;
* *Encoder Frame*: $\{x_e, y_e\}$: related to the frame of the rotary encoder installed on the test-bench. This frame can be rotated in order to be aligned according to the horizontal plane by zeroing the encoder.
* *Stages Frame*: $\{x_t, y_t\}$ related to the linear stage used to displace the magnet with respect to the coil during the in-situ calibration. The misalignment φ_t (Fig. 1) between the linear stage frame and the gravity frame induces an error on the coil phase computed during the coil in-situ calibration.

According to the measurement method of the harmonic coils [3], the 2π periodic voltage signal, resulting from the coil rotation inside the reference magnetic field, is developed into a Fourier series. The multipole field errors correspond to the Fourier series coefficients of the radial component of the magnetic flux density on the reference/measurement radius. The measured raw data are the integrated voltage signals that correspond to the flux linkage in

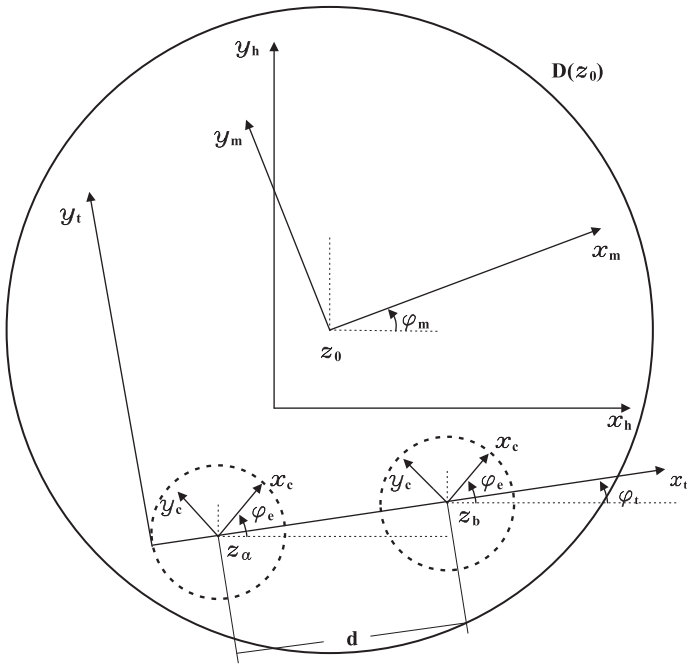

Fig. 1. Reference frames for the magnet and the measurement bench: (t) stages, (c) coil, (h) gravity, and (m) magnetic. Aperture of the calibration magnet in the disk $D(z_0)$ centered at z_0.

the coil. The stability constraints on the rotation speed are relaxed by re-parametrizing the time-domain motion into the angular position, by means of an encoder mounted on the coil shaft.

An angular uncertainty φ_e between the frames related to the encoder $\{x_e, y_e\}$ and the gravity $\{x_h, y_h\}$ must be considered (Fig. 1). If the coil shaft is equipped with a tilt-sensor, the encoder offset is zeroed by compensating the deterministic component of this angular error. The angular uncertainty φ_g between the frames of the linear stage and the coil (Fig. 1) should be considered as well, by assuming that the frames of the shaft and of the coil are coincident. The corresponding deterministic error component is assessed by reversing the magnet.

After the measurements in the two positions z_b and z_a, only the dipole $C_1 = B_1 + iA_1$ and the quadrupole components $C_2 = B_2 + iA_2$ are measured (by considering the reference magnet without higher-multipole field errors). The complex field harmonics $C_n = B_n + iA_n$ are calculated from the discrete Fourier coefficients $\widetilde{C_n}$ of flux using the coil sensitivity factors k_n. These components are expressed in the local coordinate system of the coils $\{x_c, y_c\}$.

In general, by considering all the harmonics, the two sets of measured harmonics are linked by the feed-down formula [1]:

$$C_n(z_b) = \sum_{k=n}^{\infty} C_k(z_a) \binom{k-1}{n-1} \left(\frac{\triangle z}{R}\right)^{k-n}, \tag{1}$$

where $C_k(z_a)$ are the field coefficients in z_a, $C_n(z_b)$ the field coefficients measured in z_b (after the coil translation), R the sensing-coil radius, and $\Delta z = z_b - z_a$, $|\Delta z| = d$ the displacement in the gravity frame (Fig. 1):

$$\Delta z = d e^{i\varphi_t}. \tag{2}$$

The equation relating the measured multipole field errors C_1 and C_2 in the two local coordinate systems is derived by rotating Δz into the global frame by the angle $-\varphi_e$. Then, the feed-down equation can be written as:

$$C_2(z_b) = C_2(z_a), \tag{3}$$

$$C_1(z_b) = C_1(z_a) + C_2(z_a)\frac{\mathrm{d}e^{i(\varphi_t - \varphi_e)}}{R}. \tag{4}$$

Without higher-order multipoles field errors, the feed-down does not affect the quadrupole component C_2. The systematic error of the displacement effect can be eliminated by taking the difference between the two measurements.

The multipole harmonics is not required to be known in a global reference system (e.g., the gravity frame), because the feed-down is related to the measurement at z_a:

$$R(C_1(z_b) - C_1(z_a)) = R\Delta C_1 = C_2(z_a)\mathrm{d}e^{i(\varphi_t - \varphi_e)}. \tag{5}$$

The polar representation of ΔC_1 and C_2 is made explicit:

$$R|\Delta C_1|e^{i\alpha_1} = |C_2(z_a)|e^{i\alpha_2}\mathrm{d}e^{i(\varphi_t - \varphi_e)}. \tag{6}$$

where α_1 is the phase of the variation of the component C_1 between the positions a and b, and α_2 the phase of the quadrupole component C_2 in position P_a isomorphic to z_a (Fig. 2).

Eq. (6) is fulfilled if both the modulus and the phase are equal:

$$R = \frac{\mathrm{d}|C_2(z_a)|}{|\Delta C_1|}, \tag{7}$$

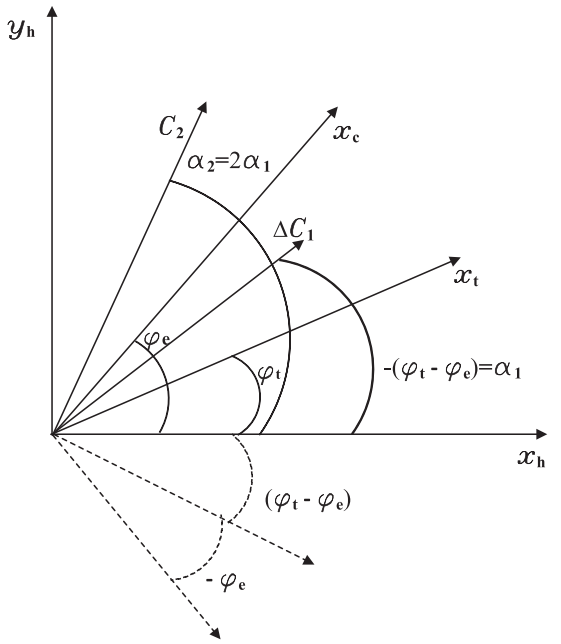

Fig. 2. Main phase angles involved in the calibration method (referred to the reference gravity frame $\{x_h, y_h\}$): α_2, phase of the quadrupole component C_2 in position p_a; φ_e, angular uncertainty of the encoder; α_1, phase of the variation of the component C_1 between the positions p_a and p_b; φ_t, misalignment of the linear stage.

$$\alpha_1 - \alpha_2 = \varphi_t - \varphi_e. \tag{8}$$

Eq. (7) gives the expression for the equivalent measurement radius of the coil.

Notice that this calibration method is independent from the alignment errors between the reference magnet and the displacement stage. The only assumption remains that the encoder error φ_e does not change between the two measurements.

Under the hypotheses of a linear translation, and the invariance of φ_e, the coil phase angle φ_c with respect to the stage frame from (6) does not change between the two measurements. Therefore, $C_1(z_b)$ and $C_1(z_a)$ have different modulus but equal phase. Furthermore, $C_2(z_a)$ has a phase angle that is double that of $C_1(z_a)$, because the magnet is a quadrupole. Thus, the condition on the phases resulting from (6) becomes:

$$\alpha_1 = \alpha_2 + (\varphi_t - \varphi_e) \tag{9}$$

where $\alpha_2 = 2\alpha_1$, thus

$$\alpha_1 = 2\alpha_1 + (\varphi_t - \varphi_e) \tag{10}$$

and if $\alpha_1 = \varphi_c$

$$\alpha_1 = \varphi_c = -(\varphi_t - \varphi_e) \tag{11}$$

$$\arg(R) = \varphi_c = -(\varphi_t - \varphi_e). \tag{12}$$

In particular, if the stage frame has been previously aligned with the gravity frame, the coil initial phase can be determined with respect to the gravity. The $\arg(R)$ is affected by rotations of the stage frame, but not of the magnet frame.

2.2. Radius calibration considering higher-order harmonics

The harmonic coils can be of the radial or tangential type, intercepting the azimuthal and the radial flux components, respectively. In the following, a radial coil is assumed, but all the developments can be applied also to tangential coils. Furthermore, consider a quadrupole containing an unwanted sextupole harmonic field error due to manufacturing errors or to variation in the remanent field of rare-earth magnets used for exciting the magnet. As an example, magnets with apertures less than 10 mm for linear accelerators show sextupole field errors in the range of 10^{-3}, while remaining still acceptable for machine installation.

In this case, the feed-down formula results in

$$\begin{aligned} C_1(z_b) &= C_1(z_a) + C_2(z_a)\left(\frac{\triangle z}{R}\right) + C_3(z_a)\left(\frac{\triangle z}{R}\right)^2, \\ C_2(z_b) &= C_2(z_a) + 2C_3(z_a)\left(\frac{\triangle z}{R}\right), \\ C_3(z_b) &= C_3(z_a), \end{aligned} \tag{13}$$

where $C_n = B_n + iA_n$. In the special case of a translation $\triangle x$ in the horizontal plane, no skew field harmonics will be excited, thus $A_n = 0$. The component $B_3(z_a)$ is therefore:

$$B_3(z_a) = \frac{1}{2}(B_2(z_b) - B_2(z_a))\left(\frac{R}{\triangle x}\right) \tag{14}$$

and,

$$B_1(z_b) = B_1(z_a) + \left(\frac{\triangle x}{2R}\right)[B_2(z_a) + B_2(z_b)]. \tag{15}$$

The relation between the coefficients obtained by Fourier analysis of the vector potential (corresponding to the flux increment per trigger signal) are related to the multipole field errors by means of the coil-sensitivity factors k_n, which depend on the number of coil turns N_t and on the coil length L. Details about the calculation of the coil-sensitivity factors are given for the radial and tangential coils in [10]. The relation between the Fourier coefficients of the vector potential $\widetilde{B}_n$ and the multipole field errors B_n is given by

$$B_n = R^{n-1}\frac{\widetilde{B}_{n+1}}{k_n}, \tag{16}$$

where

$$k_n = \frac{N_t L}{n}(R_2^n - R_1^n). \tag{17}$$

The k_n are the coil sensitivity coefficient of nth-order harmonic, R_1 is the internal coil radius, and R_2 is the external coil radius. Assuming $W = R_2 - R_1$ as the width of the coil:

$$k_1 = N_t L W = A_c \tag{18}$$

$$k_2 = N_t L W \frac{(R_1 + R_2)}{2} = A_c R \tag{19}$$

where A_c is the coil area, and R is the coil radius. The harmonic field coefficients are computed using (16):

$$B_1(z) = \frac{\widetilde{B}_2(z)}{A_c}, \tag{20}$$

$$B_2(z) = \frac{\widetilde{B}_3(z)}{A_c}, \tag{21}$$

Substituting (20) and (21) into (15) for $z = z_a, z_b$ yields:

$$\widetilde{B}_2(z_b) = \widetilde{B}_2(z_a) + \frac{1}{2}\triangle x\frac{\widetilde{B}_3(z_a)}{R} + \frac{1}{2}\triangle x\frac{\widetilde{B}_3(z_b)}{R}, \tag{22}$$

and, therefore,

$$R = \frac{\triangle x}{2}\frac{\widetilde{B}_3(z_b) + \widetilde{B}_3(z_a)}{\widetilde{B}_2(z_b) - \widetilde{B}_2(z_a)}. \tag{23}$$

A similar reasoning for an octupole component within a quadrupole magnet yields the following system of equations:

$$\begin{aligned} B_1(z_b) &= B_1(z_a) + B_2(z_a)\left(\frac{\triangle x}{R}\right) + B_4(z_a)\left(\frac{\triangle x}{R}\right)^3, \\ B_2(z_b) &= B_2(z_a) + 3B_4(z_a)\left(\frac{\triangle x}{R}\right)^2, \\ B_3(z_b) &= 3\,B_4(z_a)\left(\frac{\triangle x}{R}\right), \\ B_4(z_b) &= B_4(z_a), \end{aligned} \tag{24}$$

The coil radius can then be computed from the harmonics $\widetilde{B}_{n+1}$ of the magnetic vector potential by

$$R = \frac{\triangle x}{3}\frac{2\widetilde{B}_3(z_a) + \widetilde{B}_3(z_b)}{\widetilde{B}_2(z_b) - \widetilde{B}_2(z_a)}, \tag{25}$$

which can be generalized for any single error harmonic within a quadrupole:

$$R = \frac{\triangle x}{(n-1)}\frac{(n-2)\widetilde{B}_3(z_a) + \widetilde{B}_3(z_b)}{\widetilde{B}_2(z_b) - \widetilde{B}_2(z_a)}, \tag{26}$$

where n is the highest harmonic order, i.e., 2 for the quadrupole, 3 for the sextupole, etc.

3. Numerical results

The equations of the proposed calibration method are derived for a rotating coil with a cross section very small with respect to the spanned surface. For rotating coil to be used in very-small aperture magnets, this assumption is no more valid. Therefore, the calibration error arising from the concepts of mean surface and mean radius is analyzed by means of numerical simulation. On account of this, the CERN field computation program ROXIE [3], was used. In particular, the two case studies of a reference quadrupole with only an additional sextupole, and octupole field component were analyzed.

3.1. Presence of a sextupole field component

The actual reference magnet is modeled by means of current shells of an ideal, cos $n\Theta$, current distribution that generates a pure multipole field of order n. In particular, a sextupole current shell is nested within the quadrupole. The radii of the quadrupole and the sextupole are 70 and 50 mm. A 2D simulation is sufficient owing to the assumption of a longitudinal homogeneity both in the magnet and the rotating coil. The tangential coil section used to test the proposed method is shown in Figs. 3 and 4. During a coil rotation, 180 samples of the voltage are acquired in order to determine by Fourier coefficients of the radial magnetic flux density.

The flux linkage has been computed at two coil positions within the magnet aperture. In the first position the coil rotation axis and the magnetic axis of the calibration magnet are identical, while in the second position Fig. 3, the coil rotation center is displaced along the x-axis.

Several flux measurements were simulated using different rotating coil radii and displacements $\triangle x$ in order to check the validity of Eq. (23) for thick coils. The proposed calibration method gives more accurate and precise radius values, while the classical method (not accounting for the higher order multipole field errors.) yields errors of up to 4.5%.

Fig. 4 shows the modulus of the magnetic flux density $|B|$ of the simulated magnet obtained by overlapping an ideal quadrupole and an ideal sextupole shell magnet. The magnetic flux distribution is not symmetric and its modulus is higher on the right-hand side. The coil radius has been calculated through the classical method (without considering the higher-order multipole) in an ideal quadrupole shell magnet, for different position of coil $\triangle x$ inside the magnet aperture. These results can be compared with the case of a higher-order harmonics. The results obtained by Method 1 (see Ref. [1]) for an ideal quadrupole are shown in Table 1. These results are referred to an reference coil radius of 20 mm, as modeled in ROXIE. Results of Method 1 differ by approximately 0.11 mm mainly owing to the effect of the insulation between coil turns.

In Table 2, the results obtained using the classical (Method 1) and the proposed method (Method 2) are compared for an imposed coil radius of 20 mm in a quadrupole magnet containing an additional sextupole harmonic. These results show that the calibration error for the classical method [1] depends on the displacements $\triangle x$, while the proposed method is more robust.

3.2. Presence of an additional sextupole field component

Table 3 shows, the results obtained for a quadrupole magnet with an octupole field harmonic. The proposed method gives more accurate results than the classical one, because it takes into consideration the nonlinear radius dependence on the magnetic flux density. Obviously, the most accurate results are obtained when measurements are carried out close to the magnet center.

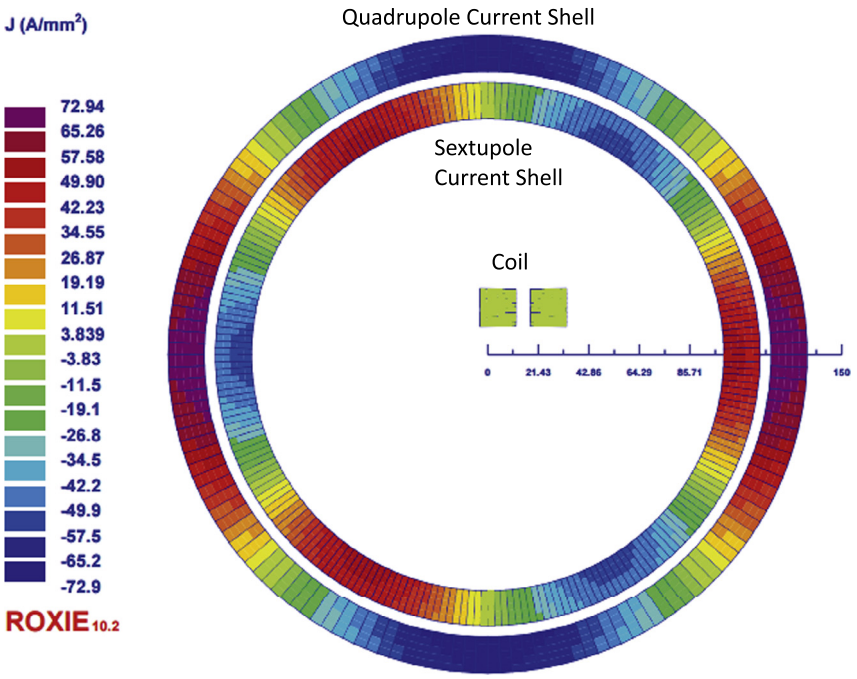

Fig. 3. Actual reference magnet modeled by ROXIE as two current shells (sextupole nested within the quadrupole) and rotating coil section (with center shifted from the magnet axis). The current density distribution J (A/mm^2) shows the asymmetry introduced by the sextupole harmonic. The induced magnetic field is magnified by ten thousand in order to display better its effect in the picture.

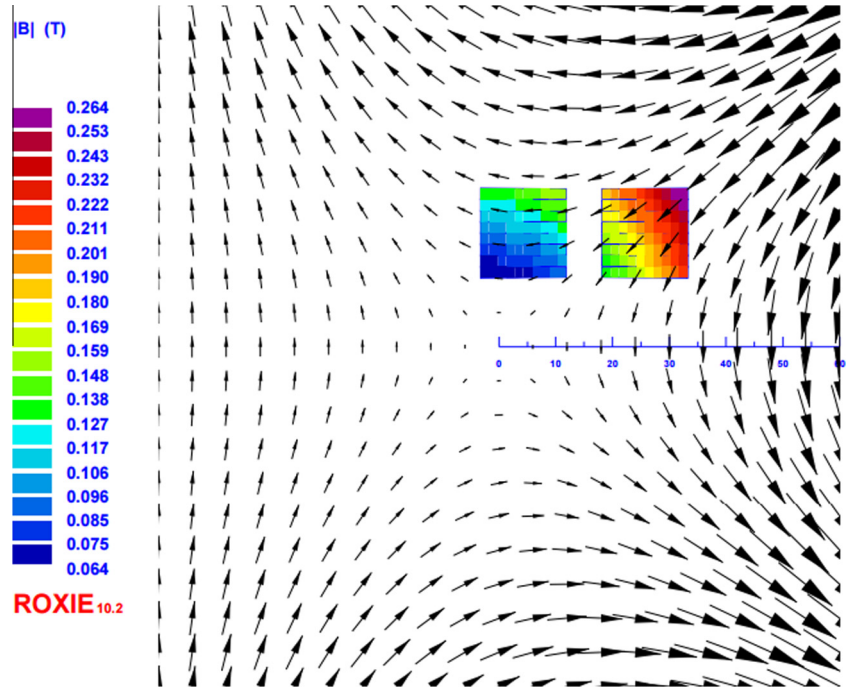

Fig. 4. Magnetic flux density in a tangential rotating coil inside the magnet aperture. The current density distribution J (A/mm^2) show the asymmetry introduced by the sextupole harmonic. The induced magnetic field is 10,000 times larger in order to display better its effect in the picture.

Table 1
Percentage accuracy of radius calibrations resulting for movements Δx from position x_1 to x_2 using Method 1, see Ref. [1], for a reference coil radius of 20.00 mm.

x_1 (mm)	x_2 (mm)	Method1 (%)
5.00	10.00	−0.55
10.00	15.00	−0.60
5.00	15.00	−0.55

Table 2
Case study of quadrupole with one additional sextupole harmonic field error: Percentage accuracy of radius calibrations for movements Δx from position x_1 to x_2, using the traditional (Method 1 [1]) and the proposed (Method 2) method, for a reference coil radius of 20.00 mm.

x_1 (mm)	x_2 (mm)	Method1 (%)	Method2 (%)
10.00	20.00	−4.50	−0.55
15.00	20.00	−2.45	−0.50
10.00	15.00	−2.55	−0.55

Table 3
Case study of quadrupole with one octupole additional harmonic: Percentage accuracy of radius calibrations resulting from movements Δx from position x_1 to x_2, with the traditional (Method 1) and proposed (Method 2) method, for a reference coil radius of 20.00 mm.

x_1 (mm)	x_2 (mm)	Method1 (%)	Method2 (%)
10.00	15.00	−1.65	−0.75
10.00	20.00	−3.40	−1.20
15.00	20.00	−2.40	−1.10

4. Experimental results

The results of the experimental validation of the proposed calibration method are reported for a case study in the test facility I8 of the Magnetic Measurement Section at CERN of a reference quadrupole magnet with a single higher harmonic of error.

4.1. Experiment setup and procedure

The experimental setup for the validation test campaign is shown in Fig. 5. The shaft is ceramic and measures 400 mm in length, with three hand-wound coils, two tangential and one for the dipole (Fig. 7a).

The test bench is equipped with a stepping motor for the coil rotation and a damper to reduce vibrations. The rotation speed is 30 rpm and the number of samples acquired per turn is 2048. The re-parametrization to the angular position is carried out by reading the trigger signals from an angular encoder, mounted on the opposite side of stepping motor. The encoder is set to zero for the coil shaft aligned with respect to the gravity, using ceramic electrolytic tilt-meter, mounted on the shaft. The magnet is displaced with respect to the coil cross section by means of a 2*D* translation stage by Physical Instruments. The data acquisition is carried out by 3 Fast Digital Integrator (FDI) [11], one for each coil. A magnet with 16-blocks of rare-earth PM material

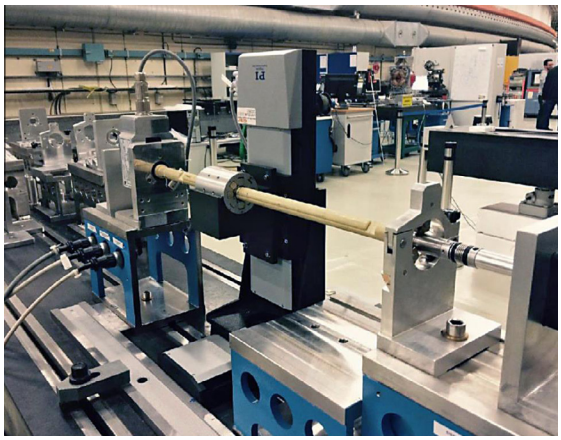

Fig. 5. Test-bench used for calibration experiment.

(Fig. 6A) was used as reference for the tests. An 8-blocks permanent magnet with an aperture of 22 mm was shimmed to create a significant sextupole harmonic (Fig. 6B). As illustrated in Fig. 6B, 3 blocks were moved towards the external side of the magnet on the left, while 3 blocks on the right were moved towards the magnet aperture.

For the calibration tests, the limited remaining space between the shaft and the magnet allowed only two steps of 0.362 mm to be carried out. The radius was calculated as the average over 7 turns both by the traditional method and by the proposed calibration with sextupole correction.

The field of the magnet does not cover all the shaft length because the shaft is longer than the magnet (Fig. 7b). During the calibration, the field of both the reference and shimmed magnets covers the same section of the rotating coil. Otherwise due to the shaft length (400 mm), the mean radius measured over the coil section covered by the magnet field could change section by section owing to the coil production errors.

4.2. Test results

The results for the two external coil rotation radius in the two magnets are compared. The results of the central coil are not considered for their higher uncertainty on the sextupole, owing to central coil smaller radius.

Table 4, the radius calibration results are reported for a movement of Δx 0.362 mm in the reference and shimmed magnets.

The results in Table 4 show that the proposed calibration with the sextupole harmonic correction performs better than the traditional method for corrections ranging from 10 to 20 μm. The sextupole harmonic introduced in the shimmed magnet is high for well-designed accelerator magnets, therefore for reference magnets with lower-amplitude higher-order harmonics, the effect of the harmonic can be neglected. On the contrary, considering the particular case of magnets with

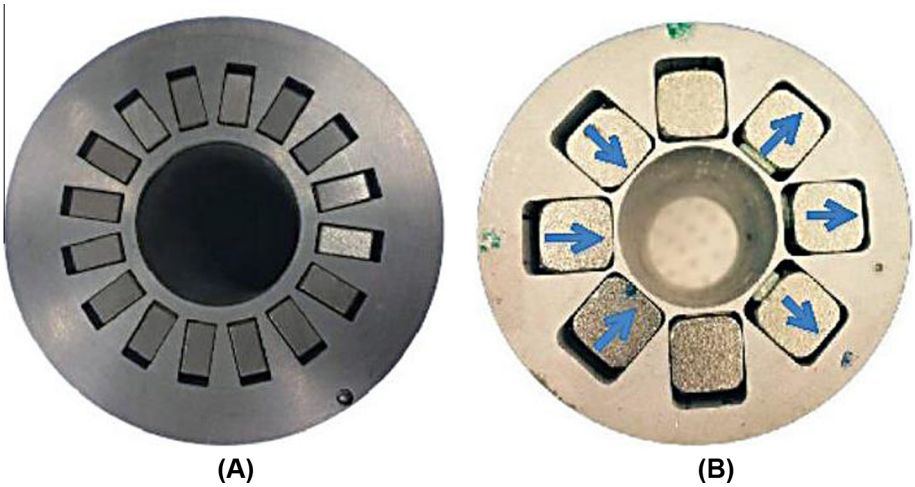

Fig. 6. (A) 16-blocks, 22-mm aperture permanent reference magnet and (B) 8-blocks, 22-mm aperture permanent magnet with additional shims to create a significant sextupole field error.

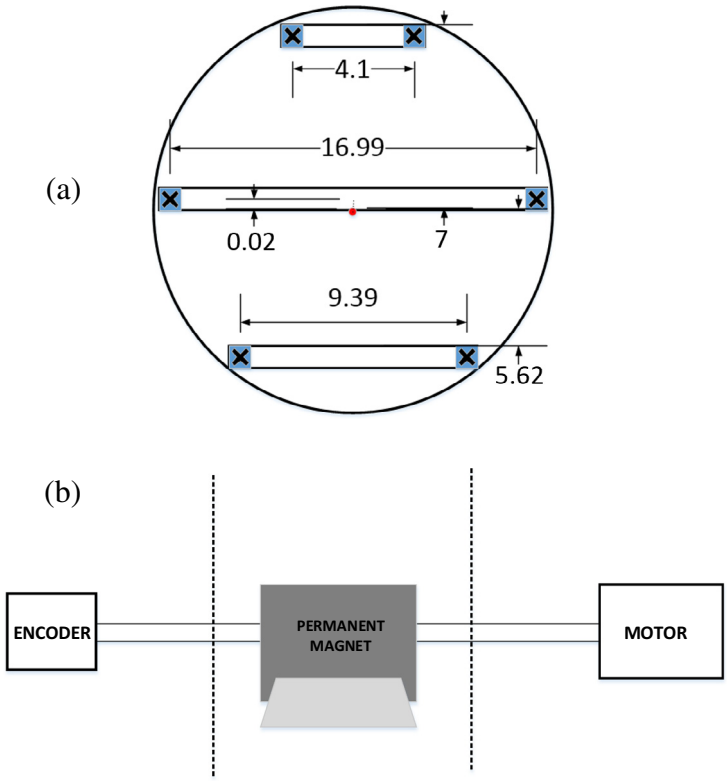

Fig. 7. (a) Rotating coil shaft sections view, the cross indicates the sections of 3 tangential coils (dimensions in mm), and (b) rotating coil test-bench longitudinal view: shaft, stepping motor and rotary encoder.

Table 4
Radius calibrations results for a movement Δx of 0.362 mm in the reference and shimmed magnets.

Magnet	Sextupole Correction	Coil 1 (mm)	Coil 2 (mm)
Reference	Yes	7.00	5.62
Shimmed	No	6.97	5.59
Shimmed	Yes	6.99	5.61

harmonic due to the assembly or to specific designs, the correction with the proposed calibration method is indeed to adopt.

The independence of the radius on the magnet frame phase was verified by repeating the calibration with the frame rotated by 45, 90, 135, and 180 degrees according to the support by using a pin. The corresponding results

Table 5
Radius calibration vs reference magnet rotation for a displacement of $\Delta x = 0.362$ mm.

Central coil (mm)	Coil 1 (mm)	Rotation (degrees)
0.043	7.00	45
0.045	6.99	90
0.044	7.00	135
0.045	6.99	180

of radius values are in Table 5. Each value is calculated according to the same displacement Δx of 0.362 mm. The proposed calibration, which consider a single higher order harmonic, gives better results with a correction of 10–20 μm.

The measured radius is stable when measured at different magnet angular positions. A variation in the order of a micrometer is present, due to the fact that is a real magnet.

5. Conclusion

A method for calibrating the rotation radius of a rotating coil sensor in a reference quadrupole magnet with a roll-angle misalignment and a significant harmonic field error or has been proposed. The method allows the metrological constraints of field quality for the reference quadrupole to be released, by allowing a wider choice of magnets to calibrate the rotating coils. Furthermore, the method can be exploited in an in-situ calibration [1] by a sextupole magnet.

Simulation results show that the worst case can yield a calibration error of 6% for a displacement of 10 mm. The results from the proposed method are accurate up to 0.1% for an additional sextupole harmonic, and up to 0.7% for the additional octupole harmonic.

Acknowledgements

The authors thank Pierre Alexandre Thonet for shimming the magnet for the experimental tests.

References

[1] P. Arpaia, M. Buzio, G. Golluccio, L. Walckiers, In-situ calibration of rotating coil magnetic measurement systems sensor coil for magnet testing, AIP Rev. Sci. Instrum. 83 (2) (2012).
[2] S. Russenschuck, O. Boine-Frankenheim, Establishing C3, the coherence between accelerator physics requirements, magnet manufacture, and magnetic measurements, in: Proc. of 20th IMEKO TC4 Symposium, Benevento, Italy, September 15–17, 2014.
[3] S. Russenschuck, Field Computation for Accelerator Magnets: Analytical and Numerical Methods for Electromagnetic Design and Optimization, Wiley, 2011.
[4] M. Buzio, Fabrication and Calibration of Search Coils, in CERN Accelerator School CAS 2009: Specialised Course on Magnets, Bruges, 16–25 June 2009, CERN, 2009.
[5] P. Arpaia, M. Buzio, J. Garcia Perez, C. Petrone, S. Russenschuck, L. Walckiers, Measuring field multipoles in accelerator magnets with small-apertures by an oscillating wire moved on a circular trajectory, IOP J. Instrum. 7 (05) (2012) P05003.
[6] L. Walckiers, Magnetic Measurement with Coils and Wires in CERN Accelerator School CAS 2009: Specialised Course on Magnets, Bruges, 16–25 June, CERN, 2009.
[7] A.K. Jain, Harmonic Coils, CERN Accelerator School on Measurement and Alignment of Accelerator and Detector Magnets, Anacapri, Italy, CERN Report 98-05.
[8] J. DiMarco, G. Chlachidze, A. Makulski, D. Orris, M. Tartaglia, J.C. Tompkins, G.V. Velev, X. Wang, Application of PCB and FDM technologies to magnetic measurement probe system development, IEEE Trans. Appl. Supercond. 23 (3) (2013).
[9] P. Arpaia, M. Buzio, G. Golluccio, L. Walckiers, A polyvalent harmonic coil testing method for small-aperture magnets, AIP Rev. Sci. Instrum. 83 (8) (2012).
[10] L. Bottura, Standard Analysis Procedures for Field Quality Measurements Part I: Harmonics, Document, LHC-M-ES-0007 Rev 1.0, CERN, 2001.
[11] P. Arpaia, L. Bottura, L. Fiscarelli, L. Walckiers, Performance of a fast digital integrator in on-field magnetic measurements for particle accelerators, AIP Rev. Sci. Instrum. 83 (2) (2012), http://dx.doi.org/10.1063/1.3673000.